Sensorimotor Rhythm as Control Signal in EEG-Based Brain-Computer Interfaces

Master's Thesis

M.E. Bol

Delft University of Technology

TU Delft

Sensorimotor Rhythm as Control Signal in EEG-Based Brain-Computer Interfaces

by

M.E. Bol

to obtain the degree of Master of Science in Mechanical Engineering
at the Delft University of Technology,
to be defended on Thursday November 9, 2023 at 10:45 AM.

Student number:	4675800	
Faculty:	Faculty of Mechanical, Maritime and Materials Engineering (3mE), Delft	
Laberatory:	NeuroMuscular Control Lab (NMClab)	
Project duration:	March 27, 2023 – November 9, 2023	
Thesis committee:	Dr. ir. M. L. van de Ruit,	TU Delft, supervisor
	Dr. ir. Y. B. Eisma,	TU Delft

An electronic version of this thesis is available at http://repository.tudelft.nl/.

TU Delft

Sensorimotor Rhythm as Control Signal in EEG-Based Brain-Computer Interfaces

M.E. Bol

Faculty of Mechanical, Maritime and Materials Engineering - Department of BioMechanical Engineering,
Delft University of Technology, Delft, The Netherlands
M.E.Bol Supervisor: M.L. van de Ruit

***Abstract*— *Background:* A brain-computer interface (BCI) is a system that enables humans to control a computer by their brain signals. This can be achieved by modulating the sensorimotor rhythm (SMR) through both motor execution and motor imagery. The potential enhancement of spinal reflexes and motor control through SMR training is attributed to the hypothesis that activity-dependent brain plasticity guides spinal plasticity during motor skill learning. However, the signal processing needed for conversion from raw brain signals to a robust control signal is challenging. The recorded electroencephalogram (EEG) signals are contaminated by multiple unknown sources and suffer from inter-subject variability, complicating the development of the BCI.**
***Objective:* To obtain a robust control signal the study 1) investigated the relation between event-related desynchronization (ERD) and mechanical stretch reflex size in the flexor carpi radialis across four muscle pre-loads consisting of 0%, 5%, 25% and 40% of maximum voluntary contraction (MVC), 2) investigated the ability of three offline signal processing paradigms in distinguishing between periods of rest and activity using EEG data associated with motor execution and motor imagery, 3) built a pseudo-online signal processing paradigm to simulate real-time signal processing based on a single trial and a continuous data stream.**
***Method:* Mechanical stretch perturbations were applied to the wrist under four percentages of MVC during motor execution and imagery conditions in six healthy subjects. The data analysis encompassed signal processing techniques including preprocessing with a large Laplacian filter, feature extraction through autoregressive modelling (AR), power spectral density (PSD), or discrete wavelet transform (DWT), and classification using linear discriminant analysis (LDA).**
***Results:* Mechanical stretch reflex sizes and ERD amplitude significantly increased with increasing percentage of MVC for motor execution trials. For motor imagery trials, no significant correlation was found between the stretch reflex size and ERD amplitude. The offline signal processing paradigms resulted in classification accuracies of 73.55% (PSD), 71.96% (DWT) and 57.13% (AR). The classification accuracies significantly increased with increasing percentage of MVC. The pseudo-online paradigm resulted in a mean classification accuracy of 51.38%.**
***Conclusions:* The EEG-based BCI shows potential for enhancing the functional recovery of patients with motor disorders. The findings demonstrate that feature extraction methods PSD and DWT could effectively distinguish between periods of rest and activity in motor execution data. Nevertheless, for the intended application, including real-time processing based on single trial motor imagery data, BCI performance should be improved. Future research should focus on motor imagery EEG data encompassing motor imagery training and feedback on motor imagery performance.**

***Keywords*— AR, BCI, DWT, Feature extraction, Motor imagery, PSD, Sensorimotor rhythm, Stretch reflex**

I. Introduction

Brain-computer interfaces (BCIs) have emerged as a product of developments in neuroscience and technology. The BCI provides a direct communication channel between the human brain and external devices. By detecting and interpreting the electrical potentials of the brain with the use of electroencephalography (EEG), BCIs can translate motor intentions of the user into commands that can be used to control an external device. BCIs make use of sensory motor rhythms (SMRs) to detect motor intention. SMRs are oscillatory events in EEG signals that arise from motor cortical brain areas associated with initiation, preparation, control and execution of the intended movement [1]. Motor preparation and execution reduce the mu oscillation (8-13 Hz) amplitude and beta oscillation (14-30 Hz) amplitude over the sensorimotor cortex, a phenomenon referred to as event-related desynchronization (ERD) [2]. As motor execution ends, the SMR increases in amplitude; a phenomenon referred to as event-related synchronization (ERS).

These ERD and ERS phenomena are also observed during motor imagery [3]. The neural activity in the sensorimotor cortex resulting from motor imagery is spatiotemporally similar to the neural activity resulting from motor execution. Motor imagery involves the imagination of the movement of a body part without carrying out physical output. There exist two types of motor imagery; visual motor imagery (VMI) and kinesthetic motor imagery (KMI) [4]. VMI involves imaging what the movement looks like. Individuals visualize themselves performing a specific motor task, thereby imaging movement details such as the trajectory and speed. While KMI involves imaging what the movement feels like, such as feeling the movement of muscles and joints involved in the movement. Several studies have demonstrated that KMI, and not VMI, modulates corticomotor excitability [5, 6]. KMI occurs in the sensorimotor area of the brain whereas VMI does not show a clear spatial pattern [7].

As BCIs operate on motor imagery, they could offer a non-invasive and non-pharmacological treatment method for individuals with neuromuscular disorders. An example of a neuromuscular disorder is spasticity which is related to hyperreflexia. The human stretch reflex is an important mechanism in the regulation of maintaining posture and muscle tone as the reflex provides a response 20-50 ms after muscle stretch onset [8]. When a mechanical stretch is applied to a muscle, two responses are typically observed in the electromyogram (EMG); the short latency M1 stretch response and the long latency M2 stretch response [9, 10]. M1 involves monosynaptic activation of alpha motor neurons. The activation leads to contraction of extrafusal muscle fibers to immediately counteract the stretch. M2 is polysynaptic as it involves both alpha motor neurons and interneurons. M2 attributes to sustained and prolonged muscle response that helps maintain muscle tone. In healthy humans, the magnitude of the neural reflex response to stretch is suggested to increase with the contraction level of the muscle until

25% of maximum voluntary contraction (MVC) after which the magnitude saturates [11, 12]. This automatic gain-scaling, where the same muscle stretch will elicit larger responses when muscle activity before the perturbation is increased, is essential [13]. Without this mechanism, the reflex response would be excessive during low contraction levels and insufficient during high contraction levels. It is believed that a disturbance in the stretch reflex may result in spasticity [14, 15]. Spasticity is a motor disorder characterized by exaggerated tendon jerks, muscle hypertonia and velocity-dependent resistance of the muscle to stretch leading to spastic movement disorders including increased reflex sizes. BCI-based SMR training might help to improve motor function recovery in people suffering from motor disorders by guiding activity-dependent brain plasticity, which is the ability of the brain to reorganize and adapt its structure in response to learning and experience [16, 17].

Understanding the relation between the SMR and the stretch reflex size across multiple percentages of MVC becomes paramount in designing effective BCIs for enhanced control. Previous studies demonstrate that the percentage of MVC influences the SMR amplitude [18, 19, 20, 21, 22]. The studies report that the SMR amplitude decreases with increasing percentage of MVC. Moreover, literature demonstrates that the SMR amplitude in the mu and beta frequency range is inversely correlated with cortical activation [23]. High SMR, corresponding to ERS, reflects synchronization of the brain rhythm which is associated with cortical inhibition. Conversely, low SMR, corresponding to ERD, is associated with cortical activation. When the SMR amplitude decreases, cortical drive to spinal motoneurons increases [24, 25]. Therefore, it is hypothesized that an increased cortical drive to motoneurons by a demanding motor task results in a smaller reflex size. In line with this hypothesis, previous studies confirm that the H-reflex is larger during rest compared to motor imagery trials [26, 27]. However, the correlation between SMR amplitude and mechanical stretch reflex size remains unclear.

To fill this knowledge gap and establish a robust control signal for EEG-based brain-computer interfaces, this study will perform a two-fold investigation. First (Experiment 1), the study will explore the potential of SMR modulation to guide stretch reflex activity by examining the impact of SMR amplitude on the stretch reflex size. The correlation between SMR, expressed in ERD amplitude, and the mechanical stretch reflex size in the flexor carpi radialis (FCR) across four muscle pre-loads consisting of 0%, 5%, 25% and 40% of MVC during motor execution and motor imagery trials will be investigated. Hypothesized is that an increase in percentage of MVC will result in an increased ERD amplitude. Moreover, it is expected that the stretch reflex size in motor execution trials will increase until 25% of MVC after which the stretch reflex size will saturate. In addition, it is hypothesized that an increase in the ERD amplitude will correspond to a reduction in the stretch reflex size in motor imagery trials. Second (Experiment 2), an offline BCI with three feature extraction methods will be implemented for offline detection of SMR amplitude modulations. The ability of three offline signal processing paradigms in distinguishing between periods of rest and activity during motor execution and motor imagery will be investigated. Signal processing of EEG data consists of three steps; pre-processing, feature extraction and classification. Pre-processing involved band-pass filtering and application of a large Laplacian filter. Feature extraction methods autoregressive modelling (AR), power spectral density (PSD) and discrete wavelet transform (DWT) were compared to one another. Linear discriminant analysis (LDA) was used as classifier. DWT takes into account both the spectral and temporal dynamics of the signal, whereas PSD exclusively focuses on spectral information and AR solely on temporal information. Therefore, it is hypothesized that feature extraction method DWT will outperform PSD and AR based on classification accuracy. In the end, a pseudo-online environment was simulated to process motor imagery EEG data in real-time to show its performance in the intended application domain including signal processing on a single trial and a continuous data stream.

The paper is organized as follows. Section II describes the methods. Section III presents the obtained results which will be discussed in Section IV. The conclusion can be found in Section V.

II. Methods

A. Subjects

Six healthy subjects were recruited for the experiments (Experiment 1: mean age 23.3 ± 0.5 y, 3 females; Experiment 2: mean age 22.0 ± 1.4 y, 3 females). Two subjects participated in both experiments. All subjects were right handed. Visual or neuromuscular impairment as well as recent injuries to the right hand or arm were specified as exclusion criteria. The subjects had no prior experience with BCIs. Prior to the experimental procedures the subjects gave informed consent. The experiments were conducted in accordance with the Declaration of Helsinki.

B. Experimental setup

Mechanical stretch perturbations were applied to the wrist by the wrist manipulator (Figure 1.a) [28]. The alignment between the axis of rotation of the wrist manipulator and the axis of rotation of the wrist ensured that a rotation of the manipulator by a certain amount of degrees resulted in an identical angular displacement of the wrist. Ramp and hold perturbations were given through the handle of the manipulator.

The EEG of the brain, the EMG of the FCR and extensor carpi radialis (ECR) and the velocity of the manipulator were recorded and sampled at 1024 Hz on a TMSi Refa Amplifier (TMSi, Odenzaal, The Netherlands). The EEG was recorded with 64 electrodes of a 128-electrode waveguard cap (Ant Neuro, Hengelo, The Netherlands). Electrodes were attached to the scalp according to the 10-10 international system. The ground electrode was fixed to the right mastoid. The EMG was recorded with four surface electrodes (CardinalHealth, Kendall 30 x 24 mm ECG electrodes H124SG). The bellies of the FCR and ECR were identified by the researcher and marked, after which the skin was cleaned with an abrasive gel and alcohol. The positive electrode was placed on the muscle belly and the negative electrode was placed near the upper insertion of the muscle. The EMG signals were band-pass filtered (20-450 Hz) prior to sampling.

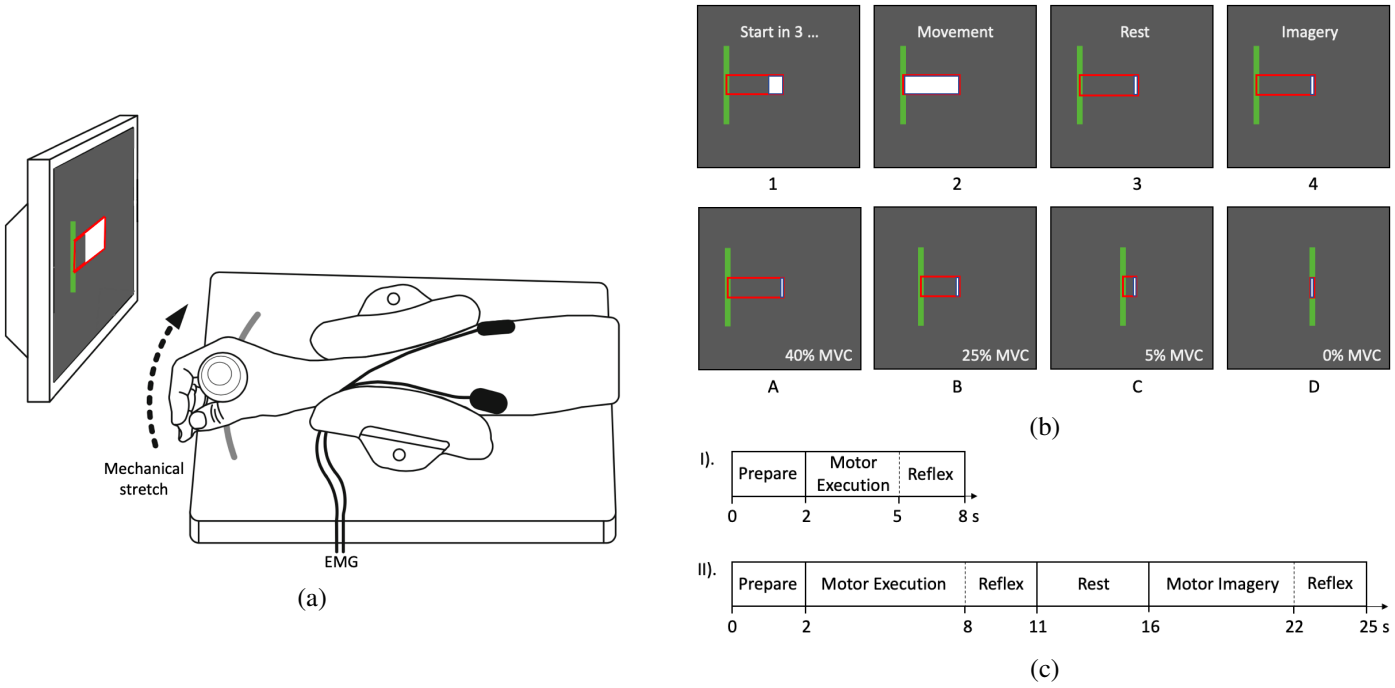

Figure 1. Experimental setup for Experiment 1 and Experiment 2. (a) Experimental setup of wrist manipulator. The displacement of the manipulator induced a mechanical stretch to the flexor carpi radialis (FCR). The mechanical stretch was applied in extension direction. The subject was asked to maintain a constant percentage of maximum voluntary contraction (MVC) by filling the red rectangular until the green line. The red block could be filled with a white color by applying force to the handle of the wrist manipulator. (b) Computer screen experiment setup. (b.1) Target appears and subject moves to target; (b.2) Target position must be held for a certain amount of time; (b.3) Rest between motor execution and motor imagery; (b.4) Subject imagines percentage of MVC without applying force to the wrist manipulator. (b.A) 40% MVC target; (b.B) 25% MVC target; (b.C) 5% MVC target; (b.D) 0% MVC target. (c.I) Movement paradigm during Experiment 1. (c.II) Movement paradigm during Experiment 2.

C. Experimental protocol

In both Experiment 1 and Experiment 2, the subjects were seated in a chair holding the handle of the manipulator with their right hand (Figure 1.a). The lower arm was fixed in an arm support to ensure alignment between the axis of rotation of the wrist and the manipulator. The subjects were positioned in front of a computer screen (Dell 19-inch LCD Monitor) on which a cursor and target were presented. An MVC measurement was performed before the start of Experiment 1 and Experiment 2. In the MVC measurement, the MVC value was determined by performing three maximum wrist flexions within a 5-second timeframe. Experiment 1 and Experiment 2 involved rest and activity tasks at multiple percentages of MVC. The subjects were instructed to perform unilateral wrist flexion by moving the cursor to a green target corresponding to either 0%, 5%, 25% or 40% of MVC starting from the wrist in its neutral position at 0° flexion (Figure 1.b). Mechanical stretch perturbations were applied during each trial. All perturbations were applied in extension direction. The perturbations were executed with an angular velocity of 2.0 rad/s and a ramp amplitude of 0.08 rad, implemented over a duration of 40 ms. No feedback of EMG or EEG data was provided to either the subject or the researcher. In the end, a second MVC measurement was conducted to assess whether the subject had experienced fatigue during the experiment. Muscle and mental fatigue were minimized by allowing sufficient rest between adjacent trials. To avoid anticipatory response, trials were pseudo-randomized and the mechanical stretch perturbations were applied at different time-intervals.

C.1. Experiment 1: Effect of MVC percentage on stretch reflex size and SMR amplitude

Experiment 1 was designed to determine the effect of 0%, 5%, 25% and 40% of MVC on the 1) SMR, expressed in ERD amplitude indicating a decrease in power of the EEG signal, and 2) stretch reflex size of the short latency M1 and the medium latency M2 reflex response in the FCR. The stretch perturbation was repeated 20 times for each of the four MVC conditions (0%, 5%, 25%, 40% of MVC), resulting in a total number of 80 trials. Step 1 and 2 of Figure 1.b were executed during Experiment 1. Experiment 1 did not contain motor imagery trials. The interval between the start of the trial and the onset of the perturbation was at randomized time between 5.0 and 8.0 s (Figure 1.c.I).

C.2. Experiment 2: Offline detection of SMR amplitude modulations by three signal processing paradigms

Experiment 2 was conducted to investigate the robustness of three signal processing paradigms. The signal processing paradigms should detect SMR amplitude modulations, which implies that the paradigms should be able to distinguish between (imaginary) activity and rest trials. Steps 1, 2, 3 and 4 from Figure 1.b were executed during Experiment 2. In contrast to motor execution trials (Figure 1.b.2), subjects were instructed to imagine the percentage of MVC on the FCR without performing wrist flexion during motor imagery trials (Figure 1.b.4). The subjects were asked to maintain the cursor at the initial position rather than moving the cursor towards the green target. No feedback on motor imagery performance

was given during motor imagery trials. The subjects used the preceding motor execution as a reference to the KMI. The stretch perturbation was repeated 30 times for each MVC condition and in both execution and imagery conditions, resulting in a total number of 240 trials. The movement paradigm is illustrated in Figure 1.c.II. The interval between the start of the trial and the onset of the perturbation was of randomized duration between 8 and 11 s for the motor execution trial and between 22 and 25 s for the motor imagery trial. To assess motor imagery ability, five visual and kinesthetic mental exercises of the Kinesthetic and Visual Imagery Questionnaire (KVIQ) [29] were performed before the start of Experiment 2. The experimenter provided the subject with imagery training and assessment instructions in accordance with the assessment procedures corresponding to KVIQ. The subject should indicate the intensity of the imagery sensation ranging from 1 (”no sensation”) to 5 (”as intense as executing the action”).

D. Data analysis

The EMG data of both Experiment 1 and Experiment 2 underwent identical processing (Section II-D.1). The offline EEG signal processing of Experiment 1 and Experiment 2 is described in Section II-D.2. Additionally, the data of Experiment 2 was used for a pseudo-online BCI simulation (Section II-D.3). Further analysis involved calculation of MVC value and KVIQ scores. The MVC value was calculated as the maximum force applied during the MVC measurement. The vividness of kinesthetic motor imagery was evaluated by summing the KVIQ scores for the five KMI questions.

D.1. EMG data processing

EMG data was processed using Matlab R2021a (The MathWorks, Inc., Natick, Massachusetts, U.S.A.) and EEGLAB 2023.0 [30]. The recorded signals (EMG and velocity of the wrist manipulator) were separated from the original data, starting 200 ms prior to and ending 150 ms after the onset of each stretch perturbation. The separated EMG segments were rectified and low-pass filtered at 80 Hz (recursive third order Butterworth filter) [31]. Each segment was normalized by the mean EMG data of the 200 ms prior to the perturbation onset of a fixed trial at 0% MVC. Segments in which the mean position of the cursor, representing the amount of muscle force, prior to onset of the perturbation deviated more than 10% of the target were rejected. Furthermore, if EMG activity was detected during 50% or more in the motor imagery time window, the EEG was contaminated and therefore excluded. The normalized segments were averaged over 20 or 30 repetitions for Experiment 1 and Experiment 2, respectively. Two metrics were derived from the rectified and normalized EMG of the FCR to quantify the M1 and M2 responses. The magnitude of the M1 response, A_{M1}, was defined as the mean amplitude of the normalized EMG in the time window between 20 and 50 ms after stretch onset. The magnitude of the M2 response, A_{M2}, was determined as the mean value of the normalized EMG between 55 and 100 ms after stretch onset.

D.2. Offline EEG data processing

EEG data was processed offline using Matlab R2021a (The MathWorks, Inc., Natick, Massachusetts, U.S.A.) and EEGLAB 2023.0 [30]. The SMR modulation was computed as described in Section D-II.2.i and Section D-II.2.ii. The data of Experiment 2 was processed with three signal processing paradigms. The offline signal processing pipeline is illustrated in Figure 2. The signal processing paradigms consisted of three steps; pre-processing (Section II-D.2.i), feature extraction (Section D-II.2.iii) and classification (Section II-D.2.iv). The three feature extraction methods included; PSD, AR and DWT. The pre-processing and classification methods were identical for the three signal processing paradigms.

D.2.i. Pre-processing

The aim of pre-processing was to enhance the signal to noise ratio by removing artifacts from the raw EEG data and reduce the effects of noise, thereby increasing the accuracy and robustness of the BCI system. As the BCI is interested in mu (8-13 Hz) and beta (14-30 Hz) rhythms, the frequency range of 1 to 40 Hz was analyzed. Pre-processing of the data involved band-pass and notch filtering. A low-pass filter (338th order finite impulse response (FIR) filter) of 40 Hz was applied to the raw EEG data, followed by downsampling to 256 Hz, a high-pass filter (846th order FIR filter) of 1 Hz and a notch filter (846th order band-pass 49-51 Hz FIR filter) at 50 Hz. Epochs were extracted starting from 3000 ms (data from Experiment 1) or 6000 ms (data from Experiment 2) before until the onset of each stretch perturbation. Electrode $C3$, positioned over the left sensorimotor cortex, was selected for further processing. The channel selection was based on the fact that SMR in the hand area of sensorimotor cortices decreases during movement planning and execution [22].

D.2.ii. ERD calculation

To detect SMR modulation between rest and multiple activity conditions, the ERD amplitude over the $C3$ electrode was computed. ERD calculation included data from Experiment 1 and Experiment 2. In addition to the pre-processing in Section II-D.2.i, common average reference (CAR) was applied as reference. The ERD was quantified by a proposed method in a previous study [2]. The calculation of ERD involved five steps: (1) band-pass filtering (subject-specific 3Hz wide frequency band, calculation see Section II-D.3.ii) of each trial, (2) squaring of amplitude samples to obtain power samples, (3) averaging of power samples over all trials, (4) averaging over time samples, (5) calculation of ERD which is described as power decrease percentage of a target period (A) to a reference period (R), (Equation 1). The target period was defined as 3000 ms (data from Experiment 1) or 6000 ms (data from Experiment 2) before until the onset of each stretch perturbation. The reference period was defined as the 3000 or 6000 ms before stretch onset during the 0% MVC condition.

$$\text{ERD} = \frac{A - R}{R} \cdot 100\% \tag{1}$$

D.2.iii. Feature extraction

The offline paradigms PSD, AR and DWT all used the same pre-processing pipeline. Additional pre-processing to Section II-D.2.i was applied before the features were extracted. A large Laplacian filter was applied to channel $C3$, where the mean activity of a set of next-nearest-neighbor electrodes was subtracted from the activity of electrode $C3$ resulting in a filtered channel $C3'$ (Equation 2). The next-nearest-neighbor

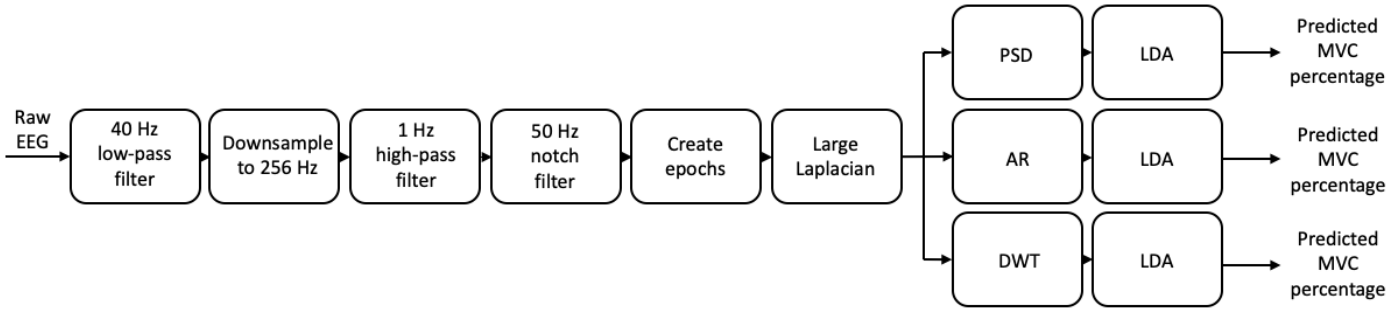

Figure 2. Three signal processing paradigms. The processing pipeline started with the raw electroencephalogram (EEG) signal. Pre-processing involved low-pass filtering, downsampling, high-pass filtering, notch filtering, extraction of epochs and large Laplacian filtering. Feature extraction methods included autoregressive modelling (AR), power spectral density (PSD), or discrete wavelet transform (DWT). The classifier employed was linear discriminant analysis (LDA) and labeled the previous obtained feature to either rest or activity. The output vector included information about the predicted state of the feature; either rest (0% of maximum voluntary contraction (MVC)) or activity (5%, 25% or 40% of MVC).

electrodes included electrodes $F3$, Cz, $P3$ and $T7$. A large Laplacian was more suited compared to a small Laplacian. A small Laplacian attenuates activity from nearest neighbor electrodes and therefore does not match the topographical extent of the control signal [32]. Furthermore, large Laplacian was chosen as spatial filter, because it outperforms CAR and ear reference based on spatial resolution and noise reduction thereby improving the accuracy of the BCI [32, 33].

$$C3' = C3 - \frac{F3 + Cz + P3 + T7}{4} \tag{2}$$

The aim of feature extraction was to extract features from the pre-processed EEG data which provided distinct properties of the signal to form a set of features on which classification could be carried out. The three feature extraction methods employed distinct from one another in the way they estimated the power spectrum of the recorded EEG signal. The non-parametric PSD is a frequency-based feature extraction method and used a Fourier transform to convert the EEG signal from time domain to frequency domain. The parametric AR analysis identified the temporal dynamics of the EEG signal by estimating autoregressive coefficients, which could then be converted to the frequency domain. DWT is a multi-resolution approach that captured both time and frequency domain information through wavelet decomposition.

1) PSD paradigm: First, an PSD algorithm was employed to estimate the mu and beta amplitude modulations. The power spectrum estimation calculated by the PSD paradigm was based on Welch averaging instead of Fast Fourier Transform (FFT) as FFT is based on linear and stationary system assumption while the brain delivers nonlinear and nonstationary signals. Welch averaging accounts for the nonstationarity by dividing the signal in multiple segments. It computes the spectral estimation for each segment using FFT and the results are averaged to obtain a smoother estimate of the PSD compared to computing the FFT of the whole signal at once.

The PSD of each epoch was calculated with the use of Welch averaging (pWelch; window length 256 samples, overlap 25% of samples). The power in a 3 Hz wide frequency band was extracted as feature. In a previous study it was demonstrated that selecting subject-specific frequency bands over fixed standard bands resulted in higher ERD detection success rate [2]. The center of the frequency band was determined with the coefficient of determination, R^2. The coefficient of determination was calculated as the squared Pearson's correlation coefficient (Equation 3), where $X(f)$ is a vector with measured EEG powers during rest and activity and $Y(f)$ is a vector with arbitrary condition labels (1, 2). Vector $X(f)$ contains the EEG power obtained from motor execution trials (90 trials; 5%, 25% and 40% of MVC times 30 repetitions) and the EEG power obtained from the rest trials (30 trials; 0% MVC times 30 repetitions) for frequency f. The correlation coefficient was determined between the conditions rest and activity over a frequency range of 0-40 Hz. A high value for R^2 at a particular frequency indicated that at this frequency the power of the EEG signal was most distinguishable between rest and activity. The frequency that corresponded to the maximum coefficient of determination was chosen as the subject-specific target frequency and used as the center of the 3 Hz wide frequency band. The features were calculated as the sum of amplitudes, by taking the square root of the power, in the subject-specific 3 Hz wide frequency band.

$$R^2(f) = \frac{cov(X,Y)^2}{var(X)var(Y)} \tag{3}$$

2) AR paradigm: Second, an AR model fitted with the Burg method was used as the algorithm to estimate the mu and beta amplitude modulations [34], similar as in a previous study [26]. Autoregressive spectral estimation was employed to estimate the power spectrum $\hat{P}(e^{j\omega})$ as in Equation 4, where $a_{p(k)}$ represents the estimated filter coefficients and p is the AR model order [35]. The model order refers to the number of prior predictions used in the model. Model order 16 was chosen as the model order, based on a literature that showed that higher model orders produced increased performance and independence in each condition [36]. The power was normalized with respect to the average power in 8-30 Hz frequency band during 0% MVC trials, similar to a previous study [27]. EEG features consisted of amplitudes within a 3 Hz wide frequency band. The 3 Hz wide frequency band of interest, which showed the most significant SMR modulation over the mu or beta band was determined with the coefficient of determination (Equation 3). The features were obtained by taking the square root of the sum of power in the 3 Hz wide subject-specific frequency band to obtain the amplitude in the band.

$$\hat{P}(e^{j\omega}) = \frac{1}{\mid 1 - \sum_{k=1}^{p} a_p(k) e^{-jk\omega} \mid^2} \tag{4}$$

Table I. Table of wavelet coefficients (approximation coefficients A_i and detail coefficients D_i) with corresponding frequency bands and EEG rhythms at different decomposition levels for Daubechies wavelet order 4 (db4) and sampling frequency of 256 Hz.

Wavelet Coefficient	Frequency Band [Hz]	EEG Rhythm
$D1$	64-128	γ
$D2$	32-64	γ
$D3$	16-32	β
$D4$	8-16	μ
$D5$	4-8	θ
$A5$	0-4	δ

3) DWT paradigm: Third, an DWT algorithm was employed to estimate the mu and beta amplitude modulations. Modulations were computed from wavelet coefficients corresponding to mu- and beta rhythm. DWT is a time-frequency feature extraction method where the signal is decomposed in a number of sub-bands at different scales depending on the number of decomposition levels. Each detail scale of the DWT corresponded to a frequency band $[f_m/2 : f_m]$, where f_m was determined by the equation $f_m = f_s/2^l + 1$. Here, f_s represented the sampling frequency and l represented the decomposition level. Wavelet decomposition of level 5 ($l = 5$) was applied to each trial. There exist several wavelet bases including Haar, Biorhogonal, Daubechies, Symlets and Coiflet. Daubechies 4 (db4) was chosen as wavelet basis, because it has been pointed out that db4 is most suitable for identifying changes in EEG signals [37, 38]. Moreover, when considering computational efficiency, the db4 wavelet stands out as the most suitable option among the available wavelet bases [39, 40]. Wavelet coefficients and corresponding sub-frequency bands obtained are displayed in Table I, where A_i represents the approximation coefficient and D_i represents the detail coefficient. The mu and beta rhythms required to identify motor execution and imagery from EEG signals are in the decomposition levels $D4$ and $D3$, respectively. The statistical features derived from these sub-bands alone were applied to the LDA classifier to identify SMR modulations. The feature vector consisted of the average power of the coefficients and standard deviation of the coefficients in every sub-band. The coefficients represented the temporal and spectral characteristics of the EEG signals in the sensorimotor regions. The average power of the wavelet coefficients represented the frequency distribution of the signal, while the standard deviation of the wavelet coefficient represented the amount of change in frequency distribution. The rows of the feature matrix were normalized using z-score normalization to ensure that each row had a mean value of zero and a standard deviation of one.

D.2.iv. Classification

LDA, also called Fisher discriminant analysis, was employed as classifier to classify the obtained features as rest (0% MVC) or activity (5%, 25%, 40% MVC) [41, 42]. The aim was to discriminate between (imaginary) activity and rest. Linear classifiers are generally more robust and need less computation time and memory compared to nonlinear classifiers such as neural networks and support vector machines. This is due to the fact that linear classifiers have less parameters to tune and are therefore less prone to overfitting. For each subject separately, the dataset was divided into test and training subsets. For the analysis, the first 40% of the dataset was used as training data. The remaining 60% of the dataset was used as testing data for the offline analysis. Only the test dataset was analyzed to evaluate the performance of the paradigm. The performance of the offline EEG signal processing paradigms was evaluated with the use of confusion matrices. The confusion matrices contained true positive (TP), true negative (TN), false positive (FP) and false negative (FN) values. Classification accuracy (ACC, Equation 5) was calculated from the values of the confusion matrices as performance metric for the offline paradigm. Classification accuracy of or above 70% is considered as the lower limit for reliable communication in BCIs [43].

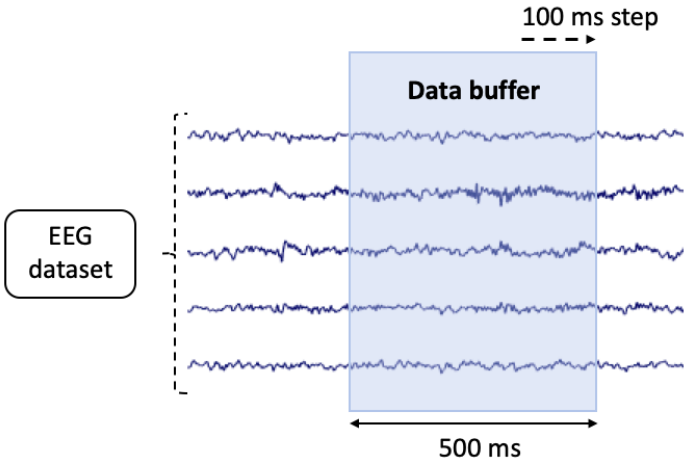

Figure 3. Illustration of simulation of pseudo-online electroencephalogram (EEG) signal processing. The data buffer contained 500 ms of EEG data. Every 100 ms the buffer moved 100 ms forward and calculated the feature value based on the previous 500 ms.

$$ACC = \frac{TP + TN}{TP + FP + FN + TN} \cdot 100\% \qquad (5)$$

D.3. Pseudo-online EEG data processing

A pseudo-online signal processing paradigm was build in Matlab R2021a (The MathWorks, Inc., Natick, Massachusetts, U.S.A.) to simulate real-time procedure in which features were extracted using continuous data to detect mu and beta amplitude modulations. The simulation of an online BCI with real-time constraints was conducted to demonstrate the performance of the paradigm in its intended application. To induce neuroplasticity, BCIs must detect movement intentions from continuous EEG signals and instantaneously generate real-time feedback. Real-time feedback is crucial as users receive information about the outcomes of their neural signals in real time, allowing them to make rapid adjustments and corrections leading to more efficient control of the BCI. A real-time robust BCI system should be able to track time, frequency and spatial nonstationarities of the EEG signal adaptively.

The feature extraction method that resulted in the highest classification accuracy in offline EEG signal processing was chosen as feature extraction method in the pseudo-online paradigm. The motor imagery EEG data from subject D, E and F from Experiment 2 was used for pseudo-online analysis. The

motor execution trials were removed, because in the intended application the BCI must operate on imagery data alone as patients may not be able to perform motor execution due to their disease. In contrast to offline processing, none of the motor imagery trials were excluded in the pseudo-online paradigm. The dataset consisted of 6 + x s periods of hand motor imagery under four MVC conditions (0%, 5%, 25%, 40%) and 5 s periods of rest. x is the time period between t = 22 s and the onset of the reflex (Figure 1.c). Each dataset contained 30 trials for each MVC condition. Two classes were defined: periods of motor imagery activity (5%, 25%, 40% MVC) and periods of rest (0% MVC and the 5 s rest period).

The pseudo-online pipeline consisted of two components; implementation of a buffer and SMR amplitude modulation detection. The EEG data was incrementally generated, in contrast to offline evaluations where the entire EEG dataset was acquired at once. Data preparation included setting up a real-time data streaming pipeline to continuously receive EEG data. A buffer was implemented to hold the incoming data and process the data in chunks. The pre-processing of the buffered data must not exceed the buffer update speed, otherwise real-time operation became impossible. Consequently, the length of the data buffer becomes a trade-off between filtering the signal uniformly and processing the signal within the time constraints of the buffer update speed. A data buffer that is too short fails to capture sufficient data to represent the entire trace. On the other hand, a long data buffer would increase computational complexity, resulting in a pre-processing time that exceeds the buffer update speed. After empirical evaluation, the buffer size was set to 500 ms. The data in the buffer was incrementally updated at the tail every 100 ms as the buffer moved forward (Figure 3). Delay in visual feedback must be below 200 ms as delays in visual feedback have been reported to degrade motor learning [44, 45]. Consequently, computational time may not exceed 200 ms. Therefore, every 100 ms, the EEG data from the previous 500 ms was processed.

The feature was calculated every 100 ms using 500 ms of data. The pre-processing was identical to pre-processing in offline environment as described in Section II-D.2.i. In addition, a large Laplacian filter on electrode $C3$ was applied on the buffered data (Equation 2). Features were extracted using PSD with the use of Welch averaging (pWelch; window length 256 samples, overlap 25% of samples) in the subject-specific 3 Hz wide frequency band. To obtain a control signal with zero mean and unit variance, the data was normalized by subtracting the mean of the previous 3 s and division by the standard deviation.

To investigate the performance of the pseudo-online paradigm, a binary threshold was implemented. The threshold was implemented offline after the pseudo-online processing. The predetermined threshold decided whether the feature represented rest or motor imagery activity. The threshold was determined by calculating the average of the power during rest in the subject-specific frequency band. The threshold was defined as $threshold = 0.8 \cdot PSD_{rest}$. The real-time binary detection results were compared with the true states to calculate the performance of the real-time EEG signal processing paradigm. The performance of the real-time processing paradigm was evaluated with the use of a confusion matrix from which classification accuracy ACC (Equation 5), precision (Positive Predictive Value (PPV), Equation 6) and sensitivity (True Positive Rate (TPR), Equation 7) were calculated.

$$PPV = \frac{TP}{TP + FP} \cdot 100\% \tag{6}$$

$$TPR = \frac{TP}{FN + TP} \cdot 100\% \tag{7}$$

E. Statistical analysis

Statistical analysis was conducted with IBM SPSS (Statistical Package for the Social Sciences) Statistics version 28.0.1.1. All data was normally distributed (by Shapiro-Wilk test, $p > 0.05$) and had equal variance (Levene's test, $p > 0.05$), therefore parametric statistical methods were utilized. The effects of MVC percentages on the stretch reflex size amplitude A_{M1} during motor imagery and motor execution trials were tested with a repeated measures analysis of variance (ANOVA). The analysis was repeated for A_{M2} stretch reflex size amplitudes. To determine if the stretch reflex size during motor imagery trials could be attributed to SMR control, the background EMG level should not be significant between the four percentages of MVC. One-way ANOVA was used as statistical measure for this task. The statistical significance of the ERD values across the four percentages of MVC was evaluated with repeated measures ANOVA for motor execution as well as motor imagery trials. To determine if a subject had experienced fatigue, a paired samples t-test was employed to determine the statistical significance of the MVC value before and after the experiment. A Pearson correlation analysis was performed to examine the correlation between the stretch reflex size amplitude and the SMR amplitude in the frequency bands. Another repeated measures ANOVA was employed to evaluate the statistical significance of classification accuracies obtained through different offline feature extraction methods, across three experimental conditions and under motor execution or motor imagery condition. Post hoc comparisons were performed using Bonferroni. A Pearson correlation analysis, between mean classification accuracy value reached by AR, PSD, DWT and corresponding KVIQ-10 KMI score, was applied to investigate whether correlation exists between offline classification accuracy for motor imagery and the reported KMI ability. For all tests, a significance level of $\alpha = 0.05$ was used.

III. Results

A total of 4% of the motor execution trials from Experiment 2 were rejected because the force prior to stretch onset deviated more than 10% of the instructed MVC target. All motor imagery trials were included as none of the trials showed more than 50% EMG activity in the motor imagery time window. The MVC value before the start of the experiment was not higher compared to the MVC value after the experiment ($p = 0.249$).

A. Stretch reflex size related to percentage of MVC

For motor execution trials, background EMG levels did significantly differ among the four percentages of MVC ($p = 0.004$). Figures 4.a and 4.b show the normalized magnitudes of M1 and M2 against the four MVC conditions, respectively. Both A_{M1} and A_{M2} significantly increased with larger percentage of MVC ($p = 0.043$, $p = 0.017$, respectively).

For motor imagery trials, background EMG levels did not differ among the four MVC conditions (p = 0.976). The normalized magnitude of M1 and M2 against the MVC conditions during motor imagery are illustrated in Figure 5. No significant relation between stretch reflex sizes, A_{M1} and A_{M2}, and percentage of MVC was found (p = 0.387, p = 0.330, respectively).

B. ERD amplitude related to percentage of MVC

Figure 6 shows the relative power, representing SMR modulations including ERD and ERS, in channel $C3$ over a subject-specific 3 Hz wide frequency band in the mu or beta rhythms under the four MVC conditions during motor execution (subject A-F) and motor imagery (subject D-F). The center of the 3 Hz wide frequency band was determined by the coefficient of determination based on data of the PSD features. For subject A the maximum coefficient of determination, R^2_{max}, value was 0.012 found at f = 9.83 Hz. The target-frequency for subject B and C was found at 9.50 Hz and 12.00 Hz, respectively. Subject D had a maximum R^2_{max} of 0.14 at a frequency of 12.83 Hz, while subject E achieved R^2_{max} of 0.34 at 14.67 Hz, and subject F obtained R^2_{max} of 0.33 at 11.83 Hz. For motor execution tasks, all subjects showed an increase in ERD amplitude as the MVC percentage increased ($p < 0.001$). Subject C showed ERS instead of ERD between 25% and 40% of MVC compared to 0% of MVC. The maximum ERD ranged between -10.69% (subject B, 40% MVC) and -58.76% (subject E, 40% MVC). The result of the motor imagery data was not significant (p = 0.273). All three subjects showed different SMR modulations during motor imagery tasks.

C. Stretch reflex size related to SMR modulation

Stretch reflex sizes during motor execution trials significantly increased with decreasing SMR amplitude. A statistically significant correlation was found between A_{M1} reflex amplitude and SMR amplitude (p = 0.012, R = -0.506). In addition, a negative correlation was found between A_{M2} and SMR amplitude (p = 0.009, R = -0.524). For motor imagery trials, no significant correlation was found between SMR amplitude and the stretch reflex sizes A_{M1} (p = 0.695) and A_{M2} (p = 0.295).

D. Performance of offline signal processing paradigms

The center of the 3 Hz wide frequency band was determined by the coefficient of determination for PSD and AR separately. Coefficients of determination and corresponding frequencies are displayed in Table II. Coefficients of determination and corresponding frequency for AR include an R^2_{max} of 0.15 at 13.00 Hz for subject D. Subject E reached an R^2_{max} value of 0.28 at a frequency of 13.00 Hz and subject F obtained an R^2_{max} value of 0.0088 at 12.00 Hz. The classification accuracies found, for the three subjects and AR, PSD and DWT signal processing paradigm, between 0%-5%, 0%-25% and 0%-40% MVC are displayed in Table III. The classification accuracy was significant across MVC conditions (p = 0.010). Pairwise comparisons using Bonferroni showed that the classification accuracy of condition 0-40% MVC was higher compared to condition 0-5% (p = 0.026). The classification accuracies were not significantly different between motor execution and motor imagery conditions (p = 0.529). In addition, classification accuracies were not significantly different between the three feature extraction methods (p = 0.409). The PSD signal processing paradigm resulted in a classification accuracy for motor execution trials of 73.55%, followed by DWT (71.96%) and AR (57.13%). For motor imagery trials, the PSD signal processing paradigm resulted in a classification accuracy of 63.31%, followed by AR (60.07%) and DWT (59.54%).

Table II. Table of coefficients of determination R^2 and corresponding target frequency f for each subject based on feature extraction methods power spectral density (PSD) and autoregressive modelling (AR).

	Subject D		**Subject E**		**Subject F**	
Method	R^2	f [Hz]	R^2	f [Hz]	R^2	f [Hz]
AR	0.15	13.00	0.28	13.00	0.0088	12.00
PSD	0.14	12.83	0.34	14.67	0.33	11.83

Table III. Table of classification accuracies for three offline signal processing paradigms during motor execution and motor imagery trials for MVC conditions 0% - 5%, 0% - 25% and 0% - 40%.

		AR		**PSD**		**DWT**	
Subject	**Condition**	Execution [%]	Imagery [%]	Execution [%]	Imagery [%]	Execution [%]	Imagery [%]
D	0-5	52.78	69.44	52.78	75.00	44.44	52.78
	0-25	63.89	75.00	66.67	66.67	69.44	63.89
	0-40	69.44	83.33	58.33	80.56	55.56	63.89
E	0-5	63.89	55.56	63.89	52.78	50.00	47.22
	0-25	38.89	52.78	75.00	50.00	86.11	61.11
	0-40	63.89	44.44	86.11	55.56	91.67	66.67
F	0-5	60.00	52.94	77.14	55.88	74.29	41.18
	0-25	47.06	57.14	94.12	65.71	88.24	71.43
	0-40	54.55	50.00	87.88	67.65	87.88	67.65
Group	0-5	58.89 ± 4.60	59.31 ± 7.24	64.60 ± 9.96	61.22 ± 9.83	56.24 ±12.96	47.06 ± 4.74
	0-25	49.88 ±10.32	61.64 ± 9.61	78.60 ±11.49	60.79 ± 7.64	81.26 ±8.41	65.48 ± 4.36
	0-40	62.63 ± 6.14	59.26 ±17.17	77.44 ±13.53	67.92 ±10.21	78.37 ±16.20	66.67 ± 1.59
	mean	57.13	60.07	73.55	63.31	71.96	59.54

E. Correlation between KVIQ score and offline classification accuracy

The KVIQ scores of subjects D, E and F are displayed in Table IV. The mean KVIQ-10 score was 35.7 out of 50. The mean KVIQ-10 score for KMI was 15.3 out of 25. The mean KVIQ-score for VMI was 20.3 out of 25. For the PSD paradigm, the classification accuracy significantly increased with increasing KMI score (R = 0.998, p = 0.040). For AR and DWT, no significant correlation was found between KVIQ-score and classification accuracies obtained (p = 0.225, p = 0.355, respectively).

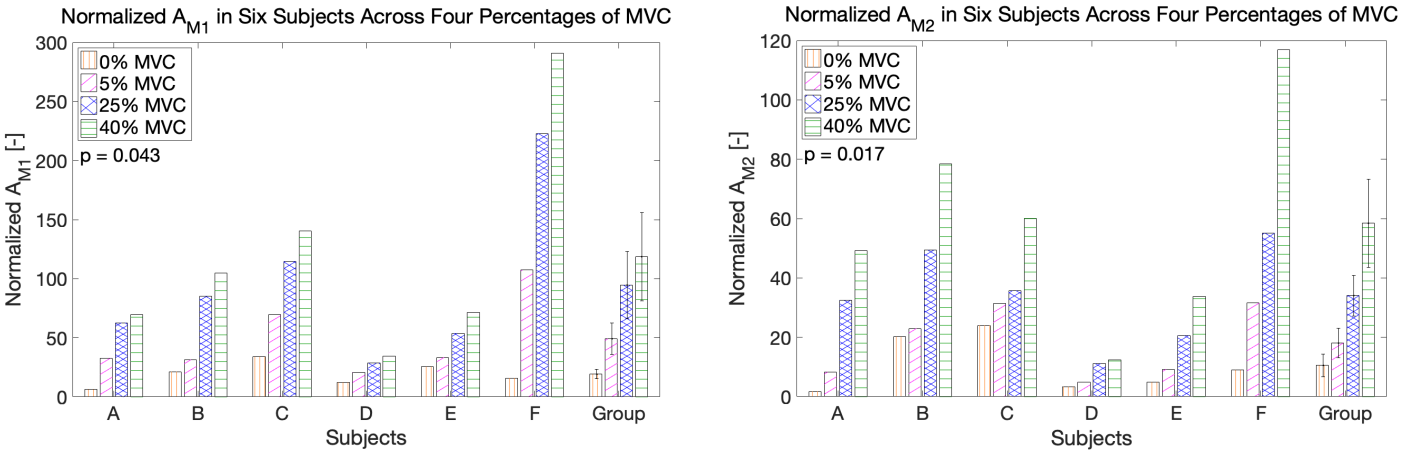

(a) (b)

Figure 4. Stretch reflex sizes of flexor carpi radialis (FCR) across four percentages of maximum voluntary contraction (MVC) during motor execution trials. (a) Normalized FCR A_{M1} stretch reflex size during 0% (yellow), 5% (pink), 25% (blue) and 40% (green) MVC in subjects (A-F) and the group average. (b) Normalized FCR A_{M2} stretch reflex size during 0% (yellow), 5% (pink), 25% (blue) and 40% (green) MVC in subjects (A-F) and the group average.

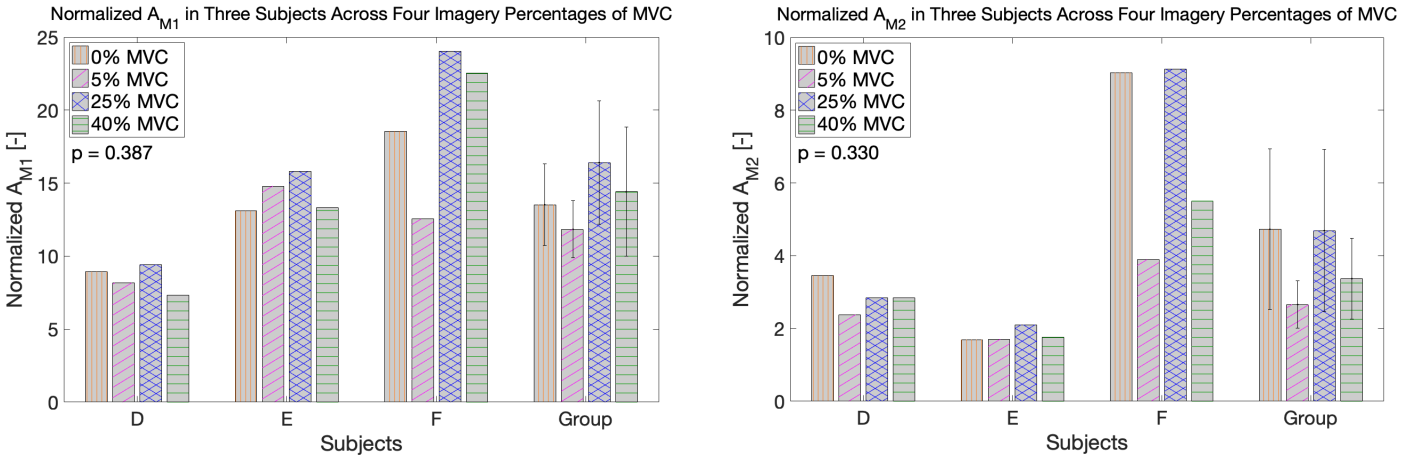

(a) (b)

Figure 5. Stretch reflex sizes of flexor carpi radialis (FCR) across four percentages of maximum voluntary contraction (MVC) during motor imagery trials. (a) FCR A_{M1} stretch reflex size during 0% (yellow), 5% (pink), 25% (blue) and 40% (green) MVC in subjects (D-F) and the group average. (b) Normalized FCR A_{M2} stretch reflex size during 0% (yellow), 5% (pink), 25% (blue) and 40% (green) MVC in subjects (D-F) and the group average.

Table IV. Table of KVIQ-scores for subjects D-F. The maximum achievable score for KVIQ-10 = 25, for KVIQ-10 KMI = 25 and for KVIQ-10 VMI = 25.

Subject	**KVIQ-10** (total = 50)	**KVIQ-10 KMI** (total = 25)	**KVIQ-10 VMI** (total = 25)
D	40	19	21
E	33	12	21
F	34	15	19
Group	35.7 ± 3.1	15.3 ± 2.9	20.3 ± 0.9

Table V. Table of online classification accuracies (ACC), positive predictive values (PPV) and true positive values (TPR) for subjects D-F and the group average.

Subject	$\boldsymbol{ACC}$ [%]	$\boldsymbol{PPV}$ [%]	$\boldsymbol{TPR}$ [%]
D	53.84	48.25	81.72
E	48.57	42.59	51.70
F	51.73	46.89	80.88
Group	51.38 ± 1.88	45.91 ± 2.09	71.43 ± 12.09

F. Performance of pseudo-online signal processing paradigm

Based on the highest achieved classification accuracy during motor imagery, PSD was chosen as paradigm for online simulation of real-time data processing. The computation time for the calculation of one feature in a buffersize of 500 ms took 7.9 ms. The classification accuracy, precision and sensitivity are displayed in Table V. The group classification accuracy (mean ± standard deviation) reached by the pseudo-online EEG signal processing paradigm was 51.38% ± 1.88. The average PPV was 45.91% ± 2.09 and the average TPR found was 71.43% ± 12.09. Figure 7 illustrates the performance of the pseudo-online paradigm. The predicted state represents the extracted feature. Features above the threshold were classified as periods of rest, while features below the threshold were classified as periods of motor imagery activity.

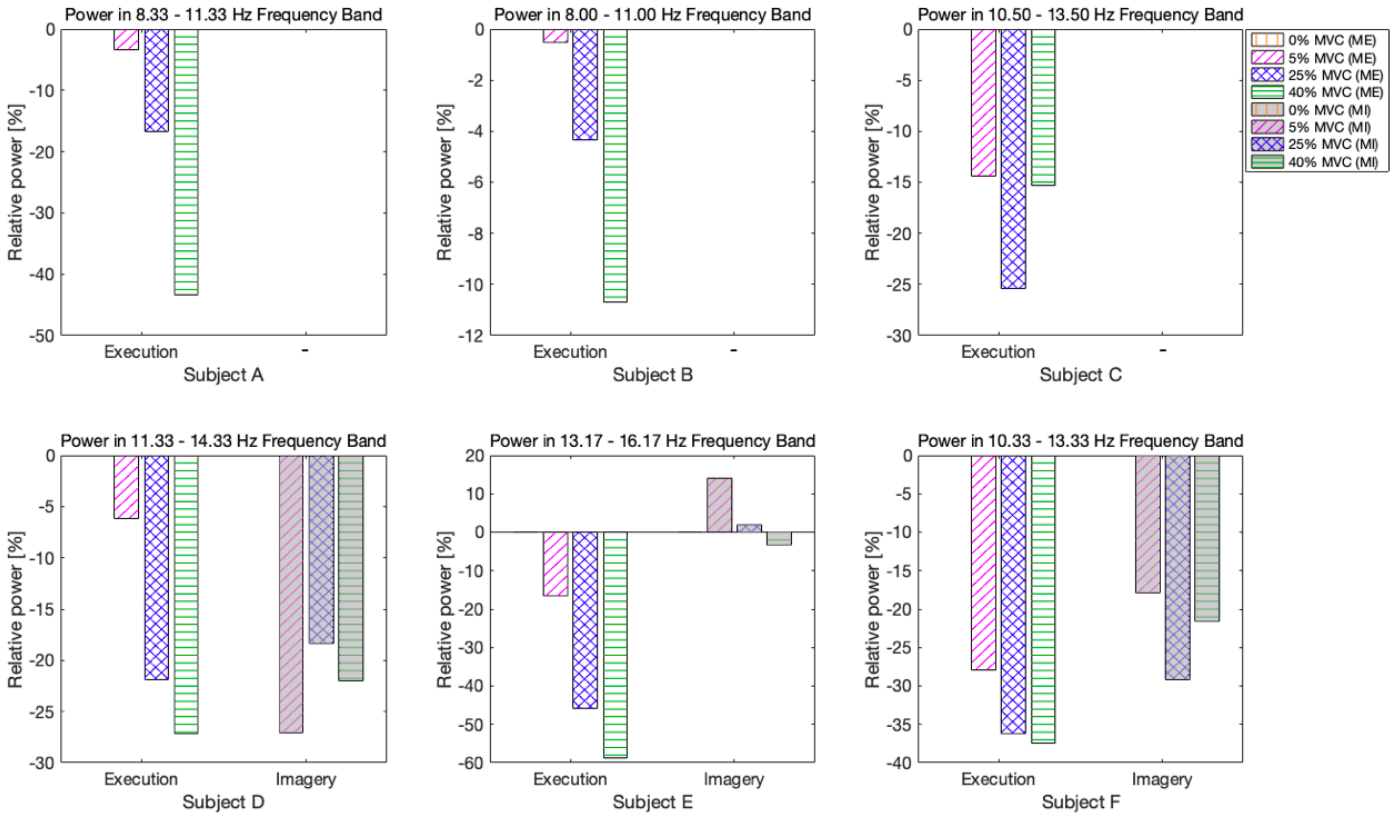

Figure 6. Event-related desynchronization (ERD) obtained from subject-specific 3 Hz wide frequency band across 0% (yellow), 5% (pink), 25% (blue) and 40% (green) of maximum voluntary contraction (MVC) during motor execution (ME) trials (subjects A-F) and motor imagery (MI) trials (subjects D-F).

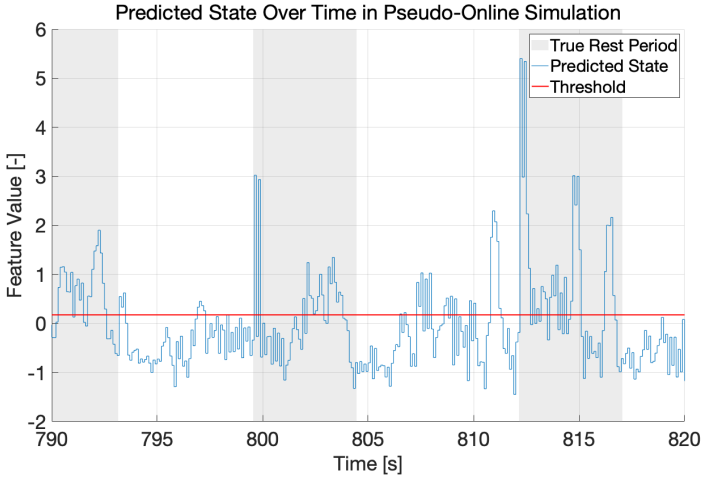

Figure 7. Chunk of simulation of pseudo-online EEG signal processing over time. Above threshold represents the rest state. Below threshold represents active state. The grey area indicates a time period in which the true condition was rest.

IV. Discussion

The aim of the study was to investigate the correlation between mechanical stretch reflex size and SMR amplitude to explore the potential of SMR modulation to guide stretch reflex activity. The mechanical stretch reflex size and SMR, expressed in ERD amplitude, across four muscle pre-loads consisting of 0%, 5%, 25% and 40% of MVC applied to the FCR for motor execution as well as motor imagery tasks were investigated. Hypothesized was that the ERD amplitude and stretch reflex size would increase with increasing percentages of MVC in motor execution trials. The study demonstrated that the stretch reflex sizes A_{M1} and A_{M2} increased with increasing percentage of MVC on the FCR (p = 0.043 for A_{M1}; p = 0.017 for A_{M2}). Furthermore, it was found that an increased MVC percentage resulted in an increase in ERD amplitude, indicating a reduction in the power of the EEG signal ($p < 0.001$). The study demonstrated that the stretch reflex size significantly increased as the ERD amplitude increased during motor execution trials (p = 0.012, R = -0.506 for A_{M1}; p = 0.009, R = -0.524 for A_{M2}). Next to motor execution data, motor imagery data was investigated. For motor imagery trials it was hypothesized that an increase in ERD amplitude would correspond to a reduction in the stretch reflex size. However, no significant relation between the stretch reflex sizes and percentages of MVC was found (p = 0.387 for A_{M1}; p = 0.330 for A_{M2}). Additionally, no significant relation was found between MVC percentage and ERD amplitude (p = 0.273). Therefore, no significant correlation was found between ERD amplitude and stretch reflex sizes during motor imagery trials. A main finding is that the hypotheses were confirmed in the context of motor execution trials but did not hold true in case of motor imagery trials.

In addition, three offline signal processing paradigms were evaluated on their ability in distinguishing between periods of rest and activity. Hypothesized was that the DWT paradigm would yield the highest classification accuracy, indicating the superior ability to extract signal features for distinguishing between rest and activity. However, classification accuracies did not differ significant between the feature extraction methods

AR, PSD and DWT (p = 0.409). Moreover, no significant distinction was found between performance of the paradigms based on motor execution or based on motor imagery data (p = 0.529). The study demonstrated that for motor execution trials, the offline signal processing paradigm PSD resulted in a classification accuracy of 73.55%, followed by DWT (71.96%) and AR (57.13%). The PSD and DWT paradigms resulted in classification accuracies above 70%, indicating that these feature extraction methods could establish a reliable communication in BCIs. For motor imagery trials, the PSD paradigm resulted in a classification accuracy of 63.31%, followed by AR (60.07%) and DWT (59.54%). Additionally, it was found that the classification accuracy increased as the percentage of MVC increased (p = 0.010). To demonstrate the performance of the PSD paradigm in its intended application, a pseudo-online signal processing method was generated to simulate real-time processing of the EEG signal. The pseudo-online signal processing paradigm resulted in a mean classification accuracy of 51.38% for a binary task.

A. Effect of MVC percentage on stretch reflex size

For motor execution trials, the baseline EMG levels exhibited a significant variation across the four MVC conditions (p = 0.004), indicating that as the MVC percentage increased, the subjects flexed their FCR muscle to a greater extent resulting in increased muscle activity. The stretch reflex sizes, A_{M1} and A_{M2}, increased significantly as the MVC percentage increased (Figure 4). This increase in reflex size when muscle activity before the perturbation is higher is a result of automatic gain-scaling. However, an increased stretch reflex size was expected up to 25% MVC, but a saturation was expected between 25% MVC and 40% MVC [11]. A previous study [46] investigated the stretch reflex of the FCR under multiple MVC percentages ranging from 5 - 95% in steps of 5%. The study showed that the group average reflex gain increased until 31% of MVC and then saturated. However, inspection of individual data of the same study revealed that reflex gain increased until 60% and then decreased at higher contraction levels. This finding is in line with our study. The absence of saturation in stretch reflex size in our study raises possibilities for increased modulation potential. The absence of saturation in stretch reflex size suggests that the neuromuscular system has not reached its upper limit of responsiveness. This lack of saturation implies that there may be room for further adaptation within the neuromuscular system. Individuals may be capable of achieving more significant levels of modulation in their muscle responses, which could be valuable for rehabilitation. The potential for increased modulation suggests that the neuromuscular system may be more adaptable and responsive to training, allowing for more effective rehabilitation outcomes.

For motor imagery trials, the baseline EMG levels did not show a significant variation across the four MVC conditions (p = 0.976) which indicates that the muscle activity was similar across the four percentages of MVC. The difference in stretch reflex size among the MVC conditions could therefore be attributed to SMR control. However, the stretch reflex size did not differ significant between percentages of MVC (Figure 5). This result implies the SMR was not modulated or did not affect the reflex size. As SMR was not modulated or did not affect the reflex size, there could not be a significant effect between stretch reflex sizes obtained from the four imaginary MVC percentages, because in motor imagery trials the pre-load of the muscle was constant across all MVC percentages.

There was considerable inter-subject variability in the reflex gains. This is likely a result of different muscle fiber compositions. The amount of fast- and slow-twitch muscle fibers in the FCR can vary due to genetic factors and training history. Moreover, inter-subject variability may have resulted from underestimation of the percentage of MVC. Fatigue did not play a role as no fatigue was experienced during the experiment, as indicated by the non-significant difference between MVC values before and after the experiment.

B. Effect of MVC percentage on ERD amplitude

The hypothesis regarding the influence of MVC percentage on the ERD is accepted for motor execution tasks, as statistical analysis revealed a significant effect of the percentage of MVC on the ERD amplitude. During motor execution, an increased ERD amplitude was observed as the MVC percentage increased (Figure 6). This decrease in EEG power indicates neural activity associated with movement. The finding aligns with the results reported in previous studies [20, 21, 22]. The variations in ERD amplitudes among subjects were anticipated, stemming from small disparities in electrode placement, impedance between the scalp and electrodes, and the extent of mu-beta modulation. It is worth noting that the results from subject C showed ERS rather than the expected ERD between the 25% and 40% MVC conditions, which contradicts the findings reported in the existing literature.

There was no significant difference found between imaging the percentages of MVC and the ERD amplitude suggesting that motor imagery has no significant influence on the ERD amplitude. As illustrated in Figure 6, the absolute ERD amplitude increased between 0% and 5% of MVC but decreased between 5% and 25% of MVC for subject D. Subject E showed ERS instead of ERD between 5% and 25% of MVC as compared to 0% of MVC. Subject F showed ERD until 25% of MVC after which the absolute ERD amplitude decreased during the 40% of MVC. This result is in contrast with a prior study where imagery of 30% of MVC resulted in a larger absolute ERD amplitude in both mu and beta rhythms compared to imagery of 10% of MVC [18]. In addition, the result is in contrast with the findings of a previous study which reported that the ERD could be observed during motor imagery and ERS during rest [3]. The finding of this study that no significant difference of ERD was found across the percentages of MVC is a result of two factors. First, the lack of training before the experiment presumably negatively affected the ERD. Previous studies showed that motor imagery training sessions did affect cortical activation patterns for healthy subjects [47, 48, 49]. Motor imagery training resulted in a stronger ERD, especially for subjects with relatively low BCI performance (classification accuracy $<$ 70%). Second, the absence of feedback during the trial could have had a negative impact on the ERD. A previous study showed that ERD was significantly larger during trials in which feedback about imagery performance was given compared to motor imagery trials without feedback [50]. In summary, the finding of a consistent ERD across the four MVC percentages in motor imagery trials is highly likely a

consequence of two critical factors: the lack of motor imagery training and the absence of feedback during the trials.

In addition to the aforementioned factors, it is worth considering the potential influence of the duration of the ERD phenomenon on the results. In previous research subjects were asked to extend their wrist and keep that position until they were told to relax after 10 seconds [51]. It was found that when the movement was sustained, the power in mu and beta bands returned to baseline values within 5 seconds. As the motor execution period and motor imagery period lasted 6 seconds in our study, it might be questioned whether the decrease in power persisted throughout the entire duration of these periods. Furthermore, another study discovered that the ERD lasted longer when subjects were tasked with a load of 130 g compared to a no-load (0 g) condition [19]. These findings may offer additional insights into why no discernible difference in ERD was observed across various percentages of MVC for motor imagery data, as opposed to motor execution data. In motor execution trials, the ERD likely did not return to baseline values within the activity time period due to the high level of muscular activity required by the task. Conversely, during motor imagery trials, it could be that ERD returned to baseline values before the end of the activity time period, because no muscular activity was required by the task. Thereby yielding no significant variation in ERD across different percentages of MVC. However, further investigation into the duration of the ERD phenomenon is needed before conclusions can be drawn.

C. Correlation between ERD amplitude and stretch reflex size

The stretch reflex size significantly increased with increasing ERD amplitude in motor execution trials (p = 0.012, R = -0.506 for A_{M1}; p = 0.009, R = -0.524 for A_{M2}). The minus sign of the correlation coefficient indicates a reduction in SMR amplitude, which in turn implies a decrease in EEG power. This decrease in EEG power corresponds to an increase in ERD amplitude. The result is in agreement with the hypothesis that ERD amplitude and stretch reflex size would increase with increasing percentages of MVC. Assumed was that motor imagery trials would yield similar effects. However, this was found incorrect. For motor imagery data, no significant correlation was found between ERD amplitude and stretch reflex size (p = 0.695 for A_{M1}; p = 0.295 for A_{M2}). The finding indicates that, in this experimental setup, motor imagery activity could not reduce the stretch reflex size of the FCR muscle. It is important to emphasize that no significant SMR modulation was found in motor imagery trials. Therefore, it is highly likely that there was no increase in cortical drive to motor neurons. Consequently, also no increase in excitation of Ia inhibitory interneurons that could have reduced the stretch reflex size. Therefore no conclusion can be drawn whether the SMR modulation could have affected the reflex size. The result is in contrast with a previous study [26] where SMR modulation affected the H-reflex size which is the electrical analogue of the stretch reflex size. The difference in results may be caused due to 10 - 30 training sessions the participants underwent prior to the experiment until they gained 80% accuracy of control over ERD and ERS. This underlines the importance of motor imagery training sessions.

D. Offline performance of signal processing paradigms

All three offline signal processing paradigms contained similar steps for pre-processing and classification of the EEG data. The feature extraction method was the only part of the calculation that differed between each paradigm. Differences in performance between the paradigms could therefore be attributed to the feature extraction method. DWT focused on both spectral and temporal information. Therefore, it was hypothesized that DWT would outperform the AR and PSD feature extraction method. However, the hypothesis did not align with the results. The classification accuracies resulting from DWT were not significantly different from AR and PSD. DWT was not significantly different from PSD likely as a consequence of the use of Welch averaging for the PSD calculation. By averaging over multiple periodograms, Welch method reduced the the variations in the signal and provided a more reliable estimate compared to traditional FFT method. The overlapping segments used in the Welch method captured the variations in the frequency content of the signal over time. Therefore, Welch method smooths over non-systematic noise and is more robust to nonstationarities compared to FFT eventually resulting in an increased performance of the PSD paradigm. Furthermore, PSD and AR extracted features from a 3 Hz wide frequency band, while DWT extracted features from wavelet coefficients $D3$ and $D4$ capturing the frequencies 8-32 Hz. DWT therefore contains more non-reactive frequency content. Illustrative is the phenomenon that when the subject showed both mu and beta modulations, DWT resulted in a higher classification accuracy compared to when a subject only showed mu modulations. Additionally, only the mean and standard deviation of the wavelet coefficients were taken into account for the feature vector of DWT. Higher order statistics such as skewness and kurtosis of the coefficients were not considered. However, it is worth noting that their inclusion, as was demonstrated in a study [52], might have resulted in a higher classification accuracy. In that study, the inclusion of skewness and kurtosis improved the classification accuracy from 64.7% to 82.0%.

Another interesting finding is that PSD resulted in a classification accuracy of 73.55% and AR in a classification accuracy of 57.13%. The outcomes for the PSD paradigm, which employed Welch averaging as the feature extraction method, align with findings from previous research [53]. Their study reported classification accuracies of 77.1% for motor execution trials and 57.3% for motor imagery trials, similar to our study (73.55% for motor execution; 63.31% for motor imagery trials). Another previous research which employed AR as feature extraction method and LDA as classifier, reported a classification accuracy of 76% [54]. AR is better suited for capturing rapid changes or variations in the signal over time, providing a higher level of detail about the temporal dynamics compared to PSD. Despite its temporal sensitivity, AR did not yield as high an accuracy as PSD. The lower classification accuracy of AR is a consequence of the coefficient of determination in which the target frequency for the 3 Hz wide frequency band is extracted. Coefficients of determination calculated with AR resulted in much lower coefficient of determination values (R^2_{mean} = 0.15) compared to PSD (R^2_{mean} = 0.27). This suggests that AR has a lower ability to distinguish between periods of rest and activity, ultimately leading to a decreased classification accuracy.

Although classification accuracies did not differ significant between feature extraction methods, it can be concluded that AR is not suitable as feature extraction method for BCI as the classification accuracy (57.13%) did not cross the lower limit for reliable communication ($ACC \geq 70\%$ [43]). The offline PSD and DWT feature extraction methods that operated on motor execution data did cross the lower limit and are therefore reliable signal processing paradigms for BCIs in an offline setting. Noteworthy, is that there was no significant difference found in classification accuracies between motor execution and motor imagery (p = 0.529). The result is in contrast with previous results of the study which showed that motor execution data showed significant SMR modulation across the MVC percentages and imagery data did not. Although the results imply that a BCI could operate on motor imagery data as effective as on motor execution data, it must be noted that the classification accuracies resulting from all feature extraction methods operating on motor imagery data resulted in classification accuracies below 70%. Indicating that the BCI could not sufficiently discriminate between activity and rest based on motor imagery data. Therefore, it cannot be concluded that BCIs work as efficient on motor imagery data as compared to motor execution data. However, if the classification accuracies of motor imagery data would be above the 70% threshold the result implies that, contrary to the conventional belief that motor imagery may not be as reliable as motor execution in motor-related tasks, the findings of this study suggest that motor imagery and motor execution data are equally effective. These findings emphasize the potential of motor imagery-based BCIs.

Variations in performance across subjects remain substantial. The variability in classification accuracies between subjects for the DWT paradigm is a result of whether the subject showed only mu modulation or also showed a peak in the beta frequency band. Subject E showed a peak in the mu and the beta frequency band resulting in a classification accuracy of 91.67% for condition 0%-40% MVC. Whereas subject D only showed a peak in the mu frequency band, thereby obtaining a classification accuracy of 55.56% for the same condition. The variability in classification accuracies between subjects for the AR and PSD paradigm holds a similar argumentation. The variations in performance are a result of the subject-specific reactive frequency band. If the subject has a distinct reactive frequency, the paradigm can easier discriminate between two states as the power at rest distinct more from activity. This is also captured in the higher value of the coefficient of determination R^2. However, if a subject does not have one strong reactive frequency, but multiple reactive bands with with smaller amplitude modulations, then it is harder to discriminate between rest and activity.

Differences between classification accuracies of different MVC conditions (0%-5%, 0%-25%, 0%-40% MVC) were found significant (p = 0.010). This result is in line with the previous found result that ERD amplitude increases as the percentage of MVC increased during motor execution ($p < 0.001$). The findings imply that it is advisable to choose 40% of MVC over 5%, resulting in an improved performance of the BCI in distinguishing between rest and activity. As the stretch reflex size did not saturate at 40% of MVC, future research should investigate the effect of ERD on the stretch reflex size at MVC percentages above 40%. Eventually, the classification accuracy might improve as the difference between ERD between rest and activity becomes larger.

Considering the effect of motor imagery ability of the subject on the performance of the BCI, it is interesting to note the difference in VMI and KMI scores (Table IV). All subjects scored higher on VMI (KVIQ-10 VMI = 20.3/25) compared to KMI (KVIQ-10 KMI = 15.3/25). This highlights the difficulty of kinesthetic imagery, eventually negatively affecting the classification accuracy results. For PSD the classification accuracy significantly increased as the KVIQ score increased (R = 0.998, p = 0.040). A similar outcome was reported in the study [6], where it was concluded that healthy individuals with higher motor imagery ability from a first-person perspective resulted in a larger magnitude SMR ERD during motor imagery. Contrary, no significant correlation was found between classification accuracies of AR and DWT and the KVIQ score (p = 0.225 for AR, p = 0.355 for DWT), similar to the outcomes in study [55] where feature extraction method Common Spatial Pattern did not show a significant correlation with KVIQ-10 scores. The results suggest that the performance of the PSD paradigm depends on the motor imagery ability of the subject, while the AR and DWT paradigm do not. Therefore, it should be questioned whether KVIQ is a reliable motor imagery assessment tool for BCI control.

The classification accuracies obtained were also affected by the choices for the classifier. It could be questioned whether single hold-out method, which samples some trials to the training set and the remaining trials to the test set, was the most optimal data resampling technique for assessing model prediction accuracy. Another resampling technique, k-fold cross-validation, samples some epochs from the dataset for the training set and the remaining for the test set. The process is iterated until every fold has functioned as the test set [56]. Next, the average of the classification accuracies is taken to obtain the classification accuracy for the signal processing paradigm. By averaging results over multiple folds, k-fold cross-validation provides a more robust estimate of model performance compared to single hold-out method.

E. Simulation of online motor imagery BCI

A pseudo-online environment was simulated to process motor imagery EEG data in real-time to show its performance in the intended application domain including processing on a single trial and a continuous data stream. The time delay for feedback to the subject would be 7.9 ms. This lag in receiving information about the outcome of the neural signals of the subject is below the threshold of 200 ms for making rapid adjustments and corrections leading to more efficient control of the BCI. This outcome suggests that, based on computational complexity, the paradigm could be implemented online. However, the classification accuracy reached by the pseudo-online paradigm was 51.38%. The result does not reject the random chance for a binary classification task. Moreover, a sensitivity of 71.43% was found, indicating that the model could relatively good identify true positives. However, the precision found was 45.91%, indicating a high rate of false positives. The model is prone to making Type I errors, where it classifies features as activity while the true state is rest (Figure

7). This performance is not desirable for implementation of a BCI for rehabilitation as the system is not reliable.

Although the frequency resolution in the online environment was higher ($f_s = 1024$ Hz) compared to offline environment ($f_s = 256$ Hz), the classification accuracy reached by PSD on imagery data in online environment (51.38%) was lower compared to offline environment (63.31%). Offline classification accuracies were higher compared to online classification accuracies, because averaging over trials was applied to get rid of variability. In the pseudo-online EEG data processing the features were calculated based on 500 ms of data. While in the offline setting, the features were calculated over 30 trials of 6000 ms each. The averaging removed the outliers thereby resulting in a higher classification accuracy compared to single-trial online EEG data processing. Furthermore, in the offline environment trials were excluded if they showed EMG activity in the time window for motor imagery and trials were excluded if the position of the cursor deviated more than 10% of the MVC target. This does not reflect the performance of a signal processing paradigm in a real-time setting. Therefore, the offline results can answer generic questions of neurophysiological interest, but are blind to the dynamics and variability to single-trial analysis methods. The study demonstrates that a certain classification in an offline environment does not indicate a similar classification accuracy in an online setting.

F. Limitations

Although, the experimental setup and procedures were chosen to obtain the desired signals and corresponding BCI performance, limitations were identified during the experiment and the data analysis. To offer refinements and opportunities for future research, limitations that may influence the interpretation of the findings will be discussed.

A limitation of the study is the small sample size, consisting of six healthy female subjects. Consequently, the results may not be generalizable to a broader population. Moreover, the study included healthy individuals and did not encompass analysis within patient populations, restricting the broader applicability of the findings to clinical contexts. In addition, this study was restricted to EEG signals originating from the left hemisphere. It is worth noting that previous research showed that left-handed individuals present weaker ERD in the mu band during motor imagery compared to right-handed individuals [57]. Therefore, to make BCI-based rehabilitation available to a wider range of individuals, it is essential to extend research to include the right hemisphere.

A constraint within the experimental setup involved that subjects were instructed to imagine the motor execution they had performed a few seconds before. This might not be suitable for the intended application. People suffering from a motor disorder might not be able to perform motor execution. Kinesthetic imagery might also be difficult if the patient was born with a motor disorder and never moved the limb voluntary. The lack on an EOG signal is another limitation of the experiment setup. Ocular artifacts could not be removed. This resulted in a distorted EEG signal, making it challenging for the classifier to detect SMR modulation. Moreover, in the online setting eyeblinks in the sliding window of the buffer could also not be detected. For future research it is recommended to stop the activity detection until the eye blink is no longer in the current sliding window in an online setting.

In the data analysis of the EEG signals, the large Laplacian filter was chosen as spatial filter, because this filter requires less electrodes compared to a CAR as spatial filter. The large Laplacian filter needs five EEG channels whereas the CAR becomes more accurate as the number of channels increases since outliers are averaged out. As the EEG signal processing paradigm is intended for real-time application where computational complexity and corresponding computation time should be below 200 ms, the large Laplacian was more suited compared to CAR. However, during several trials it occurred that one of the five channels needed for the calculation of the large Laplacian had a impedance larger than 15 kOhm, especially electrode $T7$. This was corrected during the break between the trials, but resulted in less accurate detection of the electrical potential. Another limitation in the data analysis is that it was assumed that the subject-specific 3 Hz wide frequency band was the same for motor imagery as compared to motor execution. However, since the study revealed that the ERD pattern for motor imagery trials is different as compared to motor execution trials across four MVC conditions, this assumption might be questioned. Last, no test re-test reliability was included to investigate the stability of the performance over multiple days.

All in all, it could be discussed whether motor imagery EEG-based BCIs have a potential for improving functional recovery of patients with neuromuscular disorders thereby offering a non-invasive and non-pharmacological treatment method. While motor execution trials met the hypotheses, motor imagery trials did not. Further research into the correlation between SMR and stretch reflex size during motor imagery is needed. To improve the motor imagery classification accuracy, future research should include motor imagery training sessions. In addition, future research should include feedback on the motor imagery performance during the trial. Furthermore, corticomuscular coherence should be investigated as the motor imagery EEG data did not result in similar ERD patterns as motor execution EEG data.

V. Conclusion

In conclusion, the mechanical stretch reflex size and ERD amplitude increased significantly across 0%, 5%, 25% and 40% of MVC for motor execution trials. The findings demonstrate that the stretch reflex size increases with decreasing SMR amplitude for motor execution trials. However, no significant correlation between SMR amplitude and stretch reflex size was found for motor imagery trials. In addition, three offline signal processing paradigms processed EEG data containing periods of rest and activity. A large Laplacian filter was applied for pre-processing and LDA classified the features. The offline signal processing paradigms resulted in classification accuracies of 73.55% (PSD), 71.96% (DWT) and 57.13% (AR) for motor execution trials. The PSD and DWT feature extraction method resulted in classification accuracies above 70%, indicating that these feature extraction methods were able to detect SMR amplitude modulations in an offline setting and therefore could establish a reliable communication in BCIs. The classification accuracies did not significantly differ between feature

extraction methods, but significantly increased as the MVC percentage increased. Therefore it is recommended to choose 40% of MVC over 5% to obtain an improved BCI performance. Furthermore, a simulation of the intended real-time single trial application domain resulted in a mean classification accuracy of 51.38% based on motor imagery data. It can be concluded that in theory the EEG-based BCI, that operates on a PSD or DWT signal processing paradigm on motor execution data in offline setting, could enhance the functional recovery of patients with motor disorders. Nevertheless, since these patients might not be able to perform motor execution due to their disease, and considering the real-time operational demands of the BCI, further research in real-time motor imagery performance is needed. Future research should encompass motor imagery training and real-time implementation of feedback on imagery performance to improve the classification accuracy for EEG signals resulting from motor imagery tasks.

ACKNOWLEDGEMENTS

I would like to express my appreciation to M.L. van de Ruit for his valuable insights and guidance during the research. In addition, I would like to thank the subjects for participation in the study.

REFERENCES

[1] B. Graimann, B. Allison, and G. Pfurtscheller, "Brain–computer interfaces: A gentle introduction," *Brain-computer interfaces: Revolutionizing human-computer interaction*, pp. 1–27, 2010.

[2] G. Pfurtscheller and F. L. Da Silva, "Event-related eeg/meg synchronization and desynchronization: basic principles," *Clinical neurophysiology*, vol. 110, no. 11, pp. 1842–1857, 1999.

[3] G. Pfurtscheller and C. Neuper, "Motor imagery and direct brain-computer communication," *Proceedings of the IEEE*, vol. 89, no. 7, pp. 1123–1134, 2001.

[4] Y. J. Yang, E. J. Jeon, J. S. Kim, and C. K. Chung, "Characterization of kinesthetic motor imagery compared with visual motor imageries," *Scientific Reports*, vol. 11, no. 1, p. 3751, 2021.

[5] C. M. Stinear, W. D. Byblow, M. Steyvers, O. Levin, and S. P. Swinnen, "Kinesthetic, but not visual, motor imagery modulates corticomotor excitability," *Experimental brain research*, vol. 168, pp. 157–164, 2006.

[6] H. Toriyama, J. Ushiba, and J. Ushiyama, "Subjective vividness of kinesthetic motor imagery is associated with the similarity in magnitude of sensorimotor event-related desynchronization between motor execution and motor imagery," *Frontiers in human neuroscience*, vol. 12, p. 295, 2018.

[7] C. Neuper, R. Scherer, M. Reiner, and G. Pfurtscheller, "Imagery of motor actions: Differential effects of kinesthetic and visual–motor mode of imagery in single-trial eeg," *Cognitive brain research*, vol. 25, no. 3, pp. 668–677, 2005.

[8] J. Shemmell, M. A. Krutky, and E. J. Perreault, "Stretch sensitive reflexes as an adaptive mechanism for maintaining limb stability," *Clinical Neurophysiology*, vol. 121, no. 10, pp. 1680–1689, 2010.

[9] E. Toft, T. Sinkjær, and S. Andreassen, "Mechanical and electromyographic responses to stretch of the human anterior tibial muscle at different levels of contraction," *Experimental brain research*, vol. 74, pp. 213–219, 1989.

[10] C. Ghez and Y. Shinoda, "Spinal mechanisms of the functional stretch reflex," *Experimental Brain Research*, vol. 32, pp. 55–68, 1978.

[11] J. E. Gregory, A. K. Wise, S. A. Wood, A. Prochazka, and U. Proske, "Muscle history, fusimotor activity and the human stretch reflex," *The Journal of Physiology*, vol. 513, no. Pt 3, p. 927, 1998.

[12] P. Matthews, "Observations on the automatic compensation of reflex gain on varying the pre-existing level of motor discharge in man." *The Journal of physiology*, vol. 374, no. 1, pp. 73–90, 1986.

[13] J. A. Pruszynski, I. Kurtzer, T. P. Lillicrap, and S. H. Scott, "Temporal evolution of "automatic gain-scaling"," *Journal of neurophysiology*, vol. 102, no. 2, pp. 992–1003, 2009.

[14] C. Trompetto, L. Marinelli, L. Mori, E. Pelosin, A. Currà, L. Molfetta, and G. Abbruzzese, "Pathophysiology of spasticity: implications for neurorehabilitation," *BioMed research international*, vol. 2014, 2014.

[15] L. Fu-Mei and S. Mohamed, "Correlation of spasticity with hyperactive stretch reflexes and motor dysfunction in hemiplegia," *Archives of physical medicine and rehabilitation*, vol. 80, no. 5, pp. 526–530, 1999.

[16] B. H. Dobkin, "Brain–computer interface technology as a tool to augment plasticity and outcomes for neurological rehabilitation," *The Journal of physiology*, vol. 579, no. 3, pp. 637–642, 2007.

[17] J. J. Daly and J. R. Wolpaw, "Brain–computer interfaces in neurological rehabilitation," *The Lancet Neurology*, vol. 7, no. 11, pp. 1032–1043, 2008.

[18] K. Wang, Z. Wang, Y. Guo, F. He, H. Qi, M. Xu, and D. Ming, "A brain-computer interface driven by imagining different force loads on a single hand: an online feasibility study," *Journal of neuroengineering and rehabilitation*, vol. 14, no. 1, pp. 1–10, 2017.

[19] A. Stančák Jr, A. Riml, and G. Pfurtscheller, "The effects of external load on movement-related changes of the sensorimotor eeg rhythms," *Electroencephalography and Clinical Neurophysiology*, vol. 102, no. 6, pp. 495–504, 1997.

[20] T. Mima, N. Simpkins, T. Oluwatimilehin, and M. Hallett, "Force level modulates human cortical oscillatory activities," *Neuroscience letters*, vol. 275, no. 2, pp. 77–80, 1999.

[21] C. Haddix, A. F. Al-Bakri, and S. Sunderam, "Prediction of isometric handgrip force from graded event-related desynchronization of the sensorimotor rhythm," *Journal of Neural Engineering*, vol. 18, no. 5, p. 056033, 2021.

[22] G. Pfurtscheller and C. Neuper, "Event-related synchronization of mu rhythm in the eeg over the cortical hand area in man," *Neuroscience letters*, vol. 174, no. 1, pp. 93–96, 1994.

[23] W. Klimesch, P. Sauseng, and S. Hanslmayr, "Eeg alpha oscillations: the inhibition–timing hypothesis," *Brain research reviews*, vol. 53, no. 1, pp. 63–88, 2007.

[24] M. Takemi, Y. Masakado, M. Liu, and J. Ushiba, "Event-related desynchronization reflects downregulation of intracortical inhibition in human primary motor cortex," *Journal of neurophysiology*, vol. 110, no. 5, pp. 1158–1166, 2013.

[25] C. Rau, C. Plewnia, F. Hummel, and C. Gerloff, "Event-related desynchronization and excitability of the ipsilateral motor cortex during simple self-paced finger movements," *Clinical Neurophysiology*, vol. 114, no. 10, pp. 1819–1826, 2003.

[26] A. K. Thompson, H. Carruth, R. Haywood, N. J. Hill, W. A. Sarnacki, L. M. McCane, J. R. Wolpaw, and D. J. McFarland, "Effects of sensorimotor rhythm modulation on the human flexor carpi radialis h-reflex," *Frontiers in neuroscience*, vol. 12, p. 505, 2018.

[27] M. Jarjees and A. Vučković, "The effect of voluntary modulation of the sensory-motor rhythm during different mental tasks on h reflex," *International Journal of Psychophysiology*, vol. 106, pp. 65–76, 2016.

[28] A. C. Schouten, E. de Vlugt, J. B. van Hilten, and F. C. van der Helm, "Design of a torque-controlled manipulator to analyse the admittance of the wrist joint," *Journal of neuroscience methods*, vol. 154, no. 1-2, pp. 134–141, 2006.

[29] F. Malouin, C. L. Richards, P. L. Jackson, M. F. Lafleur, A. Durand, and J. Doyon, "The kinesthetic and visual imagery questionnaire (kviq) for assessing motor imagery in persons with physical disabilities: a reliability and construct validity study," *Journal of neurologic physical therapy*, vol. 31, no. 1, pp. 20–29, 2007.

[30] A. Delorme and S. Makeig, "Eeglab: an open source toolbox for analysis of single-trial eeg dynamics including independent component analysis," *Journal of neuroscience methods*, vol. 134, no. 1, pp. 9–21, 2004.

[31] J. Schuurmans, E. De Vlugt, A. C. Schouten, C. G. Meskers, J. H. De Groot, and F. C. Van Der Helm, "The monosynaptic ia afferent pathway can largely explain the stretch duration effect of the long latency m2 response," *Experimental brain research*, vol. 193, pp. 491–500, 2009.

[32] D. J. McFarland, L. M. McCane, S. V. David, and J. R. Wolpaw, "Spatial filter selection for eeg-based communication," *Electroencephalography and clinical Neurophysiology*, vol. 103, no. 3, pp. 386–394, 1997.

[33] S. H. F. Syam, H. Lakany, R. Ahmad, and B. A. Conway, "Comparing common average referencing to laplacian referencing in detecting imagination and intention of movement for brain computer interface," *EDP Sciences*, vol. 140, p. 01028, 2017.

[34] J. P. Burg, "The relationship between maximum entropy spectra and maximum likelihood spectra," *Geophysics*, vol. 37, no. 2, pp. 375–376, 1972.

[35] D. J. Krusienski, D. J. McFarland, and J. R. Wolpaw, "An evaluation of autoregressive spectral estimation model order for brain-computer interface applications," *IEEE*, pp. 1323–1326, 2006.

[36] D. J. McFarland and J. R. Wolpaw, "Sensorimotor rhythm-based brain–computer interface (bci): model order selection for autoregressive spectral analysis," *Journal of neural engineering*, vol. 5, no. 2, p. 155, 2008.

[37] H. Adeli, Z. Zhou, and N. Dadmehr, "Analysis of eeg records in

an epileptic patient using wavelet transform," *Journal of neuroscience methods*, vol. 123, no. 1, pp. 69–87, 2003.
[38] I. Daubechies, "Orthonormal bases of compactly supported wavelets," *Communications on pure and applied mathematics*, vol. 41, no. 7, pp. 909–996, 1988.
[39] Q. Xu, H. Zhou, Y. Wang, and J. Huang, "Fuzzy support vector machine for classification of eeg signals using wavelet-based features," *Medical engineering & physics*, vol. 31, no. 7, pp. 858–865, 2009.
[40] D. Hu, W. Li, and X. Chen, "Feature extraction of motor imagery eeg signals based on wavelet packet decomposition," *IEEE*, pp. 694–697, 2011.
[41] K.-R. Muller, C. W. Anderson, and G. E. Birch, "Linear and nonlinear methods for brain-computer interfaces," *IEEE transactions on neural systems and rehabilitation engineering*, vol. 11, no. 2, pp. 165–169, 2003.
[42] B. Blankertz, G. Curio, and K.-R. Müller, "Classifying single trial eeg: Towards brain computer interfacing," *Advances in neural information processing systems*, vol. 14, 2001.
[43] E. M. Hammer, S. Halder, B. Blankertz, C. Sannelli, T. Dickhaus, S. Kleih, K.-R. Müller, and A. Kübler, "Psychological predictors of smr-bci performance," *Biological psychology*, vol. 89, no. 1, pp. 80–86, 2012.
[44] T. Honda, M. Hirashima, and D. Nozaki, "Adaptation to visual feedback delay influences visuomotor learning," *PLoS one*, vol. 7, no. 5, p. e37900, 2012.
[45] R. Schween and M. Hegele, "Feedback delay attenuates implicit but facilitates explicit adjustments to a visuomotor rotation," *Neurobiology of learning and memory*, vol. 140, pp. 124–133, 2017.
[46] I. Cathers, N. O'Dwyer, and P. Neilson, "Variation of magnitude and timing of wrist flexor stretch reflex across the full range of voluntary activation," *Experimental brain research*, vol. 157, pp. 324–335, 2004.
[47] V. Kaiser, G. Bauernfeind, A. Kreilinger, T. Kaufmann, A. Kübler, C. Neuper, and G. R. Müller-Putz, "Cortical effects of user training in a motor imagery based brain–computer interface measured by fnirs and eeg," *Neuroimage*, vol. 85, pp. 432–444, 2014.
[48] F. Pichiorri, F. D. V. Fallani, F. Cincotti, F. Babiloni, M. Molinari, S. Kleih, C. Neuper, A. Kübler, and D. Mattia, "Sensorimotor rhythm-based brain–computer interface training: the impact on motor cortical responsiveness," *Journal of neural engineering*, vol. 8, no. 2, p. 025020, 2011.
[49] J. R. Wolpaw, D. J. McFarland, G. W. Neat, and C. A. Forneris, "An eeg-based brain-computer interface for cursor control," *Electroencephalography and clinical neurophysiology*, vol. 78, no. 3, pp. 252–259, 1991.
[50] C. Neuper, R. Scherer, S. Wriessnegger, and G. Pfurtscheller, "Motor imagery and action observation: modulation of sensorimotor brain rhythms during mental control of a brain–computer interface," *Clinical neurophysiology*, vol. 120, no. 2, pp. 239–247, 2009.
[51] F. Cassim, W. Szurhaj, H. Sediri, D. Devos, J.-L. Bourriez, I. Poirot, P. Derambure, L. Defebvre, and J.-D. Guieu, "Brief and sustained movements: differences in event-related (de) synchronization (erd/ers) patterns," *Clinical neurophysiology*, vol. 111, no. 11, pp. 2032–2039, 2000.
[52] J. Kevric and A. Subasi, "Comparison of signal decomposition methods in classification of eeg signals for motor-imagery bci system," *Biomedical Signal Processing and Control*, vol. 31, pp. 398–406, 2017.
[53] D. Huang, K. Qian, S. Oxenham, D.-Y. Fei, and O. Bai, "Event-related desynchronization/synchronization-based brain-computer interface towards volitional cursor control in a 2d center-out paradigm," *IEEE*, pp. 1–8, 2011.
[54] R. Yang, D. A. Gray, B. W. Ng, and M. He, "Comparative analysis of signal processing in brain computer interface," *IEEE*, pp. 580–585, 2009.
[55] V. Peterson, C. Galván, H. Hernández, and R. Spies, "A feasibility study of a complete low-cost consumer-grade brain-computer interface system," *Heliyon*, vol. 6, no. 3, p. e03425, 2020.
[56] C. Beleites, U. Neugebauer, T. Bocklitz, C. Krafft, and J. Popp, "Sample size planning for classification models," *Analytica chimica acta*, vol. 760, pp. 25–33, 2013.
[57] D. Zapała, E. Zabielska-Mendyk, P. Augustynowicz, A. Cudo, M. Jaśkiewicz, M. Szewczyk, N. Kopiś, and P. Francuz, "The effects of handedness on sensorimotor rhythm desynchronization and motor-imagery bci control," *Scientific reports*, vol. 10, no. 1, p. 2087, 2020.